A Simple Closed-Form Expression For Calculation Of The Electrospun Nanofiber Diameter By Using ABC Algorithm

Cagdas Yilmaz, Deniz Ustun, Ali Akdagli

Abstract: The producing of nanofiber tissue scaffolds is quite important for enhancing success in tissue engineering. Electrospinning method is used frequently to produce of these scaffolds. In this study, a simple and novel expression derived by using artificial bee colony (ABC) optimization algorithm is presented to calculate the average fiber diameter (AFD) of the electrospun gelatin/bioactive glass (Gt/BG) scaffold. The diameter of the fiber produced by electrospinning technique depends on the various parameters like process, solution, and environmental parameters. The experimental results previously published in the literature, which include one solution parameter (BG content) as well as two process parameters (tip to collector distance and solution flow rate) related to producing of electrospun Gt/BG nanofiber, have been used for the optimization process. At first, the AFD expression has been constructed with the use of the solution and process parameters, and then the unknown coefficients belonging to this expression have been accurately determined by using the ABC algorithm. From 19 experimental data, 15 ones are used for the optimization phase while the other 4 data are utilized in the verification phase. The values of average percentage error between the calculated average fiber diameters and experimental ones are achieved as 2.2 % and 5.7 % for the optimization and verification phases, respectively. The results obtained from the proposed expression have also been confirmed by comparing with those of AFD expression reported elsewhere. It is illustrated that the AFD of electrospun Gt/BG can be accurately calculated by the expression proposed here without requiring any complicated or sophisticated knowledge of the mathematical and physical background.

Index Terms: Artificial bee colony algorithm, Bioactive Glass, Electrospinning, Gelatin, Modeling, Nanofibers, Tissue scaffold

1 INTRODUCTION

The bone ensuring mechanical support to the body has a very complex structure and it is a mineral reservoir. Moreover, the bone helps muscular contraction resulting in motion and safeguards internal organs [1]. The bone tissue may be damaged at different rates by causing of the various reasons. The bone tissue, which is slight bone damage can repair itself in a few weeks without requiring any intervention [2]. If the bone tissue has a severe bone damage caused by diseases of the trauma, malignancy, infections, and congenital, it can be reconstructed by using autograft, allograft or biocompatible material [3]. Autograft is that the healthy tissues of the patient transferred to the damaged area of the own body. In autograft, it is non–toxic, histocompatible and well–suited for bone regeneration because the tissue source is the patient itself. But, autograft may cause morbidity at the donor site after harvesting of the tissues. Also, the healthy tissue of elders may not be sufficient for this process at sometimes. On the other hand, allografts which provided from the human cadavers or living donors can occur the undesired immunological rejections. Tissue engineering has emerged as a promising approach to overcome these shortcomings [4]. The primary components of this approach are tissue scaffolds, functional cells, and signals (provided chemically by growth factors or physically by a bioreactor) [5]. Extracellular matrix (ECM) is a structural support for cells and it assistances the cells to perform many vital functions like cell adhesion, cell-to-cell communication, cell growth, proliferation, differentiation, and etc. [6].

- *Cagdas Yilmaz, Mersin University, Faculty of Engineering, Department of Electrical–Electronics Engineering, Mersin, Turkey, PH-(+90) 324 361 0001. E- mail: bmmcagdas@gmail.com*

The aim of tissue engineering is to provide the most similar environment to a natural extracellular matrix with the help of the signal added tissue scaffold for the cells that will produce the target tissue. Thus, the tissue formed by cells that have suitable conditions can be transferred to patients. The matchless mechanical properties of the natural bone are provided by the successful design of structures that are in ranging size of micro to nano [7]. Bone is a composite consisting of 70 % mineral and 30 % organic. While a very large portion of the mineral part consists nanoscale hydroxyapatite (HA) crystals, the organic part includes glycoproteins, sialoproteins, and collagen. The majority of the bone matrix structure is formed from the HA crystals. The HA crystals are generally 20–80 nm long and 2–5 nm thick [8]. Other parts except for HA also consist nanometer size. For example, type I collagen, which is the main component of the organic part (over 90 %) is about 280–300 nm long and 1.5 nm in diameter [9]. It is seen that the cells are largely surrounded by nanosized structures in their natural environment and they directly interact with nanostructured ECM that consists nanofiber. The experiments proved that the nanostructured scaffolds are more successful than macro-structured ones, thanks to performing more amounts of specific protein interaction in stimulating bone growth. Researches also show that these nanostructured scaffolds also are effective in vital cell functions such as proliferation, migration, differentiation, and the creation of natural ECM [7, 10, 11]. Because of these reasons, nanoscale scaffold production is extremely significant for tissue engineering. In order to produce scaffolds with nanofibers, various techniques like self–assembly, phase separation, and electrospinning are used. Among these, electrospinning is the most popular method because of a wide range of natural and synthetic materials can be produced besides it is simple and inexpensive [12, 13]. Electrospinning applies a high-voltage electric field to form solid fibers from a polymeric fluid jet given with millimeter-scale nozzle. This method capable of producing scaffolds which mimic features of the natural bone matrix structure. Electrospinning can produce nanofiber having high

porosity, high aspect ratio, and large surface area. Furthermore, this method can produce fibers with diameter size varying from nanometers to micrometers [14]. The choice of appropriate material is one of the most important stages in the production of the tissue scaffold. It should not be forgotten that the characteristic of the selected material influences severely overall features of the tissue scaffold [15]. Because of the extracellular matrix of the bone tissue consists of inorganic and organic materials, all the features of an ideal tissue scaffold are not possible to obtain by using a single material. Therefore, the usage together of materials with different properties instead of using only one kind of materials provides the producing of tissue scaffolds with better mimic capable [2]. Gelatin (Gt) is a natural, biocompatible and biodegradable material and the structure of Gt is very similar to bone. The Gt having these properties mentioned above frequently uses in tissue engineering [16]. Bioactive glass (BG) which having attractive properties like bioactivity, osteoconductivity and its ability to form a strong bond with bone and soft tissues, is another commonly used material in tissue engineering [17]. The composite material obtained by using gelatin together with bioactive glass provides an addition benefits in tissue engineering due to utilizing the both Gt and BG advantages [18]. The fiber diameter fabricated by using electrospinning method is dependent on some parameters as process variables, solution variables and environmental conditions. The process variables include the applied voltage, flow rate of the polymer solution, tip to collector (TTC) distance, needle diameter, collector type and etc. The solution variables consist of molecular weight of the polymer, the concentration of polymer solution, viscosity, conductivity, solvent type and etc. while the environmental conditions occur temperature, humidity, and pressure [19]. The determining of fiber diameter is extremely important since the fiber diameter effects the mechanical, electrical, optical of the nanofibers [20, 21]. Response surface method (RSM) is a practical modeling method applying together mathematical and statistical methods intended for understanding and analyzing the existing relationship between electrospinning parameters and diameters of fibers fabricated by using electrospinning method [22, 23]. As an estimating tool, the method of artificial neural networks (ANNs) has been successfully applied to different engineering problems and tasks. Several studies are available in the literature for calculation of produced electrospun fiber diameter by using RSM and ANN [22, 24-28]. Pezeshki-Modaress et al. [27] used RSM for predicting the diameters of gelatin/chitosan fibers. Gelatin/chitosan blend ratio, the applied voltage and flow rate have used as input parameters for the model. In [24], ANN is employed to predict the electrospun gelatin fiber diameter with an acceptable error. Khanlou et al. [22] utilized both RSM and ANN for predicting the diameters of electrospun polymethyl methacrylate (PMMA) fibers. It was reported that the method of ANNs is superior to RSM in terms of error percentage and correlation coefficient factor. However, in another study [25] in which both ANN and RSM have been used for modeling the average diameter of electrospun polyacrylonitrile (PAN) fibers, it was concluded that RSM is more successful than ANN. As a composite material, Gt/BG is widely used by the researchers to produce tissue scaffolds [29-31]. In [19], a model obtained by using RSM for calculating the fiber diameter of electrospun Gt/BG is presented. The above methods based on ANN and RSM can be used with their own limitations and merits, however, ANN does not give any information about the relative importance of various parameters in the problem considered due to computing in a black box. As a collection of mathematical and statistical techniques developed for an empirical model, RSM may not accomplish the most proper results. Therefore, the simpler, ready to use and more accurate expressions regarding (Gt/BG) as well as the other composites are still required for the researchers in tissue engineering. In this study, a novel and simple closed-form expression depending on the process and solution parameters like BG content, flow rate, and TTC distance is empirically derived by using the artificial bee colony (ABC) algorithm for accurate calculation of the average fiber diameter (AFD) of electrospun Gt/BG. The ABC algorithm [32-35] based on the swarm intelligence is developed by mimicking the behavior of the honey bees for exploring the nectar sources. The paper is organized as follows: the ABC algorithm is explained in Sections 2. The derivation of the diameter expression is given in section 3. The numerical results obtained in this work are presented in Section 4 while the conclusion is given in Section 5.

2 ARTIFICIAL BEE COLONY ALGORITHM

Lately, the subject of the swarm intelligence has been increased the attraction as a research interest for many scientists in various areas. The swarm intelligence can be described as any shared information about the foods between each other individual in the swarm by the collective behavior of insects and other animal societies. The approach the swarm intelligence can become the inspiration for researchers to design algorithms or distributed problem–solving devices. The ABC method [32-35] developed by inspiring by the intelligent foraging behavior of honey bee swarms is a recently proposed optimization algorithm based on the swarm intelligence. The artificial bee colony consists of three groups as employed bees, onlooker bees, and scout bees. The employed bees are the half of the colony and its number is equal to nectar sources around the hive. The second half includes the onlooker bees and its population number are also equal to the number of employed bees. The employed bees randomly fly to find the food source positions representing optimal solutions in a multidimensional search space and the food source positions determined by the employed bees are recorded in their memory. Then, they dance to share information about that food sources with the onlooker bees waiting in the dance area at the hive. The best food sources from those found by the employed bees are preferred by onlooker bees and the onlooker bees adjust their position by considering information including the nectar amounts of the food sources. The food sources are exhausted by the employed bee and then the employed bee becomes a scout bee to search further food sources once again. The ABC algorithm pseudocode is illustrated below:

Initialization step:

1. Initialize the population of solutions x_{ij}

$$x_{ij} = x_j^{\min} + rand(0,1) \cdot (x_j^{\max} - x_j^{\min}) \quad (1)$$

Here, *i=1, 2, …, FS; j=1,2, …, D*. Where, *FS* and *D* indicate the number of food sources and the dimension of the optimization parameters, respectively.

2. Evaluate nectar amount (fitness) of the food sources.
3. Iteration=1

Repeat

Employed bees step: Employed bees go to the food sources and detect their amounts.

4. Generate new solutions (*food source positions*) v_{ij} in the neighborhood of x_{ij} for the employed bees using the formula given below.

$$v_{ij} = x_{ij} + \phi_{ij}(x_{ij} - x_{kj}) \quad (2)$$

Here, $k \in 1, 2, \ldots, FS$ and $j \in 1, 2, \ldots, D$ are randomly selected indices. Although k is detected randomly, it has to be dissimilar. ϕ_{ij} is a random number between [–1, 1].

5. Apply the greedy selection process between x_{ij} and v_{ij}.

***Onlooker bees step*:** The onlooker bees calculate the probability value of the sources.

6. Compute fitness values to minimize problems using the following equation:

$$f_{it_i}(x_{ij}) = \begin{cases} \dfrac{1}{1 + f_{it_i}(x_{ij})} if \cdots f_{it_i}(x_{ij}) \geq 0 \\ 1 + abs(f_{it_i}(x_{ij})) if \cdots fit_i(x_{ij}) < 0 \end{cases} \quad (3)$$

7. The probability value pi with which x_{ij} is selected by an onlooker bee can be computed by the expression given:

$$f_{it_i}(x_{ij}) = \frac{f_{it_i}(x_{ij})}{\sum_{n=1}^{FS} f_{it_i}(x_{ij})} \quad (4)$$

Normalize p_i values into [0,1].

8. Generate the new solutions (new positions) v_i for the onlookers from the solutions x_i, chosen depending on p_i, and evaluate them.
9. Apply the greedy selection process for the onlookers between x_i and v_i

Scout bees step: If a source is abandoned by an employed bee, the scout bee is randomly sent to search the area for discovering new food sources.

10. Detect the abandoned solution (*source*), if it exists, and replace it with a new randomly produced solution x_i for the scout bee using the "(1)"
11. Memorize the best food source position (*solution*) achieved so far.
12. Cycle=Cycle+1.

Finalization

Until cycle=Maximum Cycle Number (*MCN*)

The shape illustrating the flow of the ABC algorithm is given in Fig. 1. At the initial phase, the values of possible solution concerning the food source locations randomly generate between two specified limitation values in the search space. The fitness (*Nectar amount or food quality*) of the generated values with respect to the amounts of the food is calculated to judge the profitability in the first step. In the onlooker bees phase, the probability of the possible solution values is computed by using values of their fitness and the onlooker bees and the bees search new possible solutions around food positions having values with high probability. In the scout bees phase, if a possible solution point never improves after a specified number of trial limits, a new possible solution is randomly produced by a scout bee like the generating process of a possible solution in the initial step. Finally, the best solution point obtained for each phase is memorized. These phases sequentially continue until defined the *MCN*.

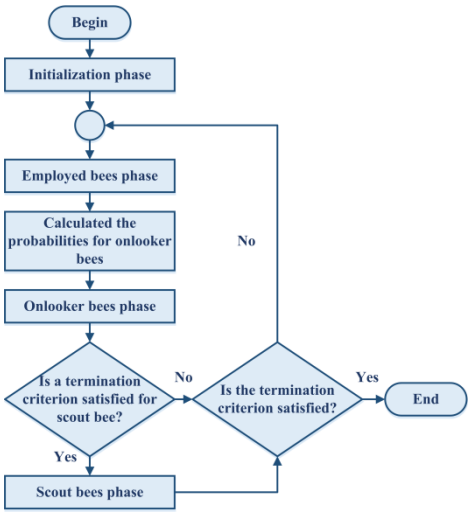

Fig. 1. *The flow chart of the ABC algorithm*

3 THE DERIVATION OF THE AVERAGE FIBER DIAMETER EXPRESSION

In order to construct the expression for AFD of the Gt/BG tissue scaffold, 19 experimental data reported in [19] have been used. In the optimization process, while 15 samples are used for the expression construction phase, the remainder 4 samples are left for the verification phase. The ranges of the process and solution parameters used in the experiments and the experimental results for the fiber diameter of Gt/BG tissue scaffold are given in Table 1 and Table 2, respectively. Note that, BG consisting of 45 % SiO_2, 24.5 % Na_2O, 24 % CaO, 6 % P_2O_5 and 0.5 % CuO is produced by [19] with the use of the classical melting method. Details on the preparation of BG powders and composite fibers can be found in [19].

TABLE 1

THE RANGES OF THE PROCESS AND SOLUTION PARAMETERS USED IN THE EXPERIMENTS [19]

Process and solution parameters	Range	
	Minimum	Maximum
BG content (wt %)	5	7
Flow rate (mL/h)	1	3
TTC distance (cm)	7	10

TABLE 2

THE EXPERIMENTAL RESULTS FOR THE FIBER DIAMETER OF GT/BG TISSUE SCAFFOLD [19]

Experimental Number	Experimental process and solution parameters			AFD (nm)
	X BG content (wt %)	Y Flow rate (mL/h)	Z TTC distance (cm)	
1	5	1	8.5	658±191
2	7	1	8.5	505±96
3	5	3	8.5	491±81
4	7	3	8.5	625±168
5	5	2	7.0	465±69
6	7	2	7.0	616±157
7	5	2	10.0	489±110
8	7	2	10.0	516±103
9	6	1	7.0	610±128
10	6	3	7.0	534±114
11	6	1	10.0	585±144
12	6	3	10.0	594±111
13	6	2	8.5	523±84
14	6	2	8.5	527±87
15	6	2	8.5	561±134

For simplicity; BG content, flow rate, and TTC distance are denoted as X, Y and Z, respectively. The unknown coefficients of the expression including these electrospinning parameters are optimally determined by the agency of the ABC algorithm so as to minimizing the following average percentage error (*APE*).

$$APE = \frac{\sum_{k=1}^{EN}\left[\left|\frac{AFD_{\exp_k} - AFD_{cal_k}}{AFD_{\exp_k}}\right| \times 100\right]}{EN} \quad (5)$$

where AFDexp and AFDcal are the experimental and calculated fiber diameter values, respectively. The EN is the number of the experiment. The optimization parameters of ABC used in this work and their assigned values are given in Table 3.

TABLE 3

THE OPTIMIZATION PARAMETERS USED IN THE ABC ALGORITHM

Parameters	Assigned values
Number of dimensions (D)	11
Population size (NP)	50
Maximum iteration number	3000
Trial number	NP*D

In order to find the best model corresponding the AFD, a number of trials are carried out. The following AFD expression which is producing satisfactorily results is obtained.

$$AFD = a_1 \cdot \frac{M}{N} \quad (6.a)$$

$$M = a_2 \cdot X^{a_3} + Y^{a_4} + Z^{a_5} + a_6 \cdot X \cdot Y + a_7 \cdot Y \cdot Z + a_8 \cdot X \cdot Z \quad (6.b)$$

$$N = a_9 \cdot Y^{a_{10}} + a_{11} \cdot Z^{a_3} + a_{12} \cdot X^{a_3} \cdot Y \cdot Z^{a_3} + a_{13} \cdot Y^{a_3} \cdot Z + a_{14} \cdot X \cdot Y^{a_3} \cdot Z^{a_3} \quad (6.c)$$

Note that the AFD expression models which were simpler and more complicated than that given by "(6)" were also tried. The simpler models were not in good agreement with the experimental results, and, the more complicated models provide little improvement in the APE value. In Table 4, the coefficient values obtained by using ABC algorithm for considering 15 experiment samples are listed.

TABLE 4

COEFFICIENT VALUES FOR AFD EXPRESSION DETERMINED BY THE ABC ALGORITHM

a_1	a_2	a_3	a_4	a_5	a_6	a_7
46,55	-2,86	2	5,61	2,521	49	-29,37
a_8	a_9	a_{10}	a_{11}	a_{12}	a_{13}	a_{14}
-0,32	3,987	3	0,1413	0,00244	-0,878	-0,00224

Fig. 2 is given the convergence rate of the ABC algorithm. It can be clearly seen that the convergence speed of the ABC algorithm is remarkable. Although the proposed model has high degree of nonlinearity it took about 3 minutes by a personal computer running at 2.4 GHz with 4 GB RAM.

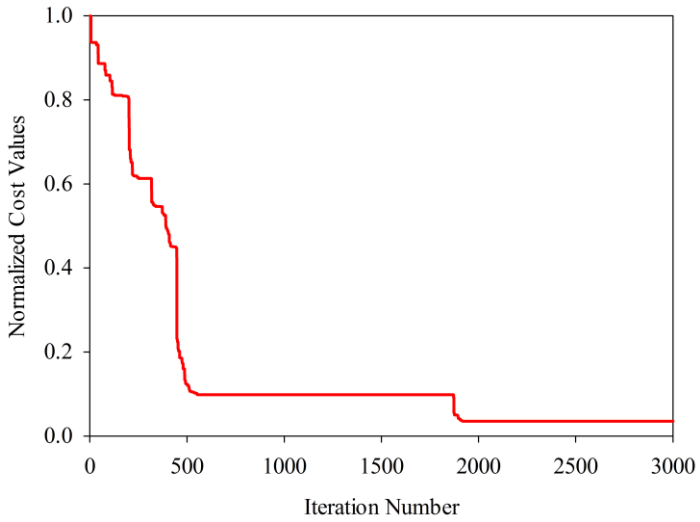

Fig. 2. *The convergence rate of the ABC algorithm*

4 NUMERICAL RESULT

The results of AFD for 15 samples for calculated by using the proposed expression are tabulated in Table 5. This table also contains the results of AFD expression presented in [19]. The whole AFD results are given in Table 5 and Fig. 3 so as to compare with each other clearly. It is evident from Fig. 3 and Table 5, both the expressions yield the remarkable results, however, our calculated AFD values agree well with the experimental ones. Average Percentage Error (APE) and Total Absolute Error (TAE) are achieved as 2.2 % and 206, respectively for 15 experiments, and this good agreement supports the accuracy of AFD formula proposed in this work. The parameters values of 4 experimental samples and the calculated AFD for each sample are given in Tables 6 and 7, respectively. In order to verify the validity and fidelity, the reminder 4 experimental samples are also examined in the AFD formula, and, APE and TAE are obtained as 5.7 % and 118, respectively.

TABLE 5

COMPARISON OF EXPERIMENTAL AND CALCULATED AFD VALUES

AFD (nm)			Error (%)	
Experimental	Calculated			
[19]	This study	[19]	This study	[19]
658	593	641	9,88	2,58
508	508	539	0,00	6,10
491	491	470	0,00	4,28
625	573	652	8,32	4,32
465	465	482	0,00	3,66
616	616	585	0,00	5,03
489	489	534	0,00	9,20
516	516	512	0,00	0,78
610	598	617	1,97	1,15
534	534	545	0,00	2,06
585	585	564	0,00	3,59
594	560	577	5,72	2,86
523	527	528	0,76	0,96
527	527	528	0,00	0,19
561	527	528	6,06	5,88
APE (%)			2.2	3.5
TAE	206	288		

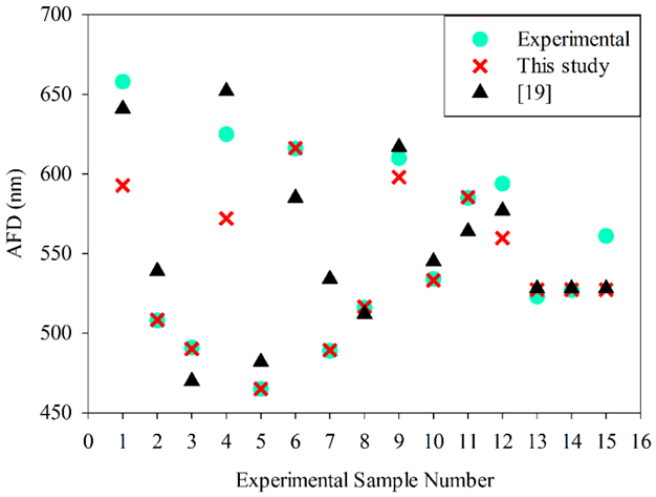

Fig. 3. *The comparative results of the calculated and experimental AFD*

TABLE 6

THE PARAMETERS VALUES OF THE 4 EXPERIMENTAL SAMPLES USED FOR VERIFICATION PHASE

Parameters		
BG content (wt %)	Flow rate (mL/h)	TTC distance (cm)
7	1	10
7	3	10
5	1	7
5	3	7

TABLE 7

COMPARISON OF EXPERIMENTAL AND CALCULATED AFD VALUES FOR VERIFICATION PHASE

AFD (nm)			Error (%)	
Experimental	Calculated			
[19]	This study	[19]	This study	[19]
526	517	482	1,6	8,4
514	574	637	11,6	23,9
599	600	636	0,1	6,18
527	478	423	9,3	19,73
APE (%)			5,7	14,6
TAE	118	308		

Further to investigate the individual effect of the BG content, flow rate, and TTC distance, two parameters are fixed to their corresponding average values, and changing the calculated AFD over the third one is depicted in Fig. 4. Fig. 4.a shows AFD versus BG content while flow rate and TTC distance values are fixed. As seen, once BG content increases, AFD increases as well. In Fig. 4.b, the curve of AFD with respect to flow rate is illustrated, and it looks like a sine waveform. It indicates that AFD has maximum and minimum values around 2.5 and 1.5 ml/h of flow rate. As the last task of the parametric studies is performed for TTC distance. The variation of AFD with respect to TTC distance is shown in Fig. 4.c and it was seen that as TTC distance is increasing the corresponding AFD is decreasing, in general.

(a)

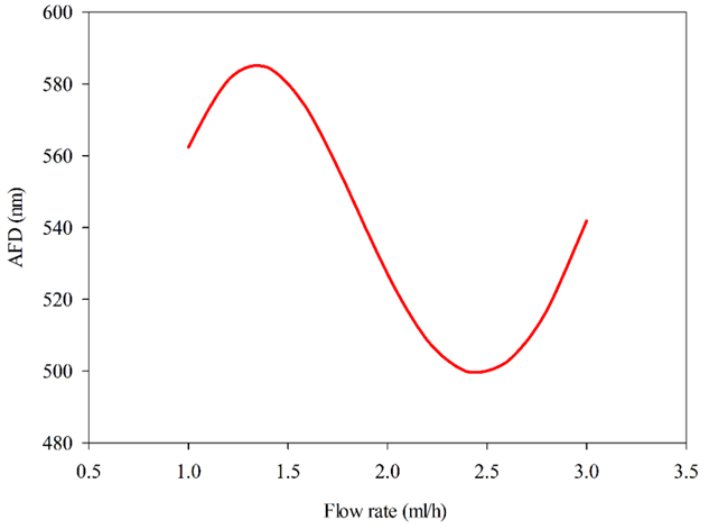

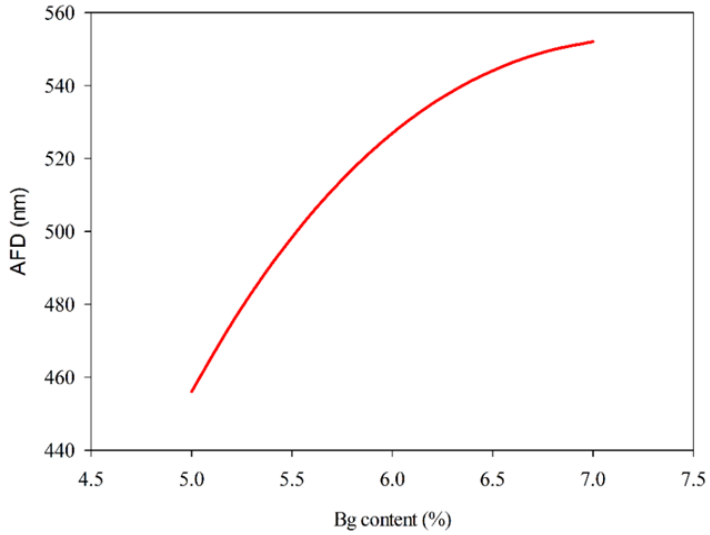

(b)

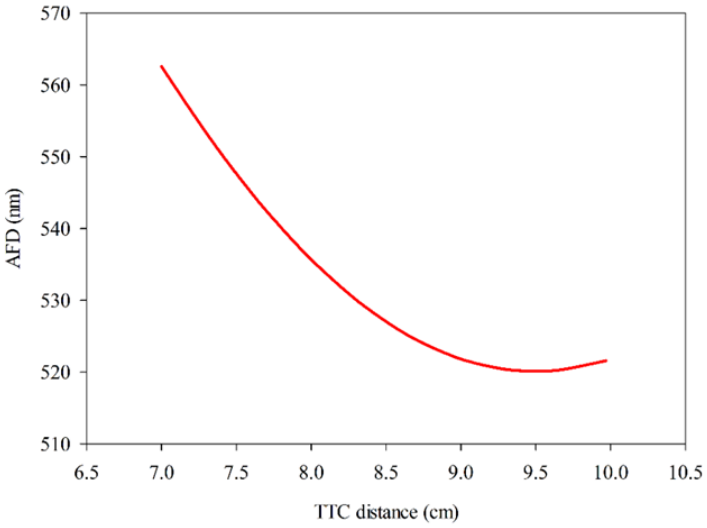

(c)

Fig. 4. *The variation of AFD with respect to a) BG content b) Flow rate c) TTC distance*

5 Conclusion

In the presented study, a novel and robust expression calculating the AFD of electrospun Gt/BG fiber has been proposed. A total of 15 experiments having different electrospinning process parameters such as BG content (wt %), TTC distance, and Flow rate has utilized to derive the fiber diameter expression. The results computed from the expression obtained by using the ABC algorithm have been compared with the other ones derived by using RSM reported elsewhere, and it was shown that the expression provides better results in terms of experimental ones. It is concluded that due to the simplicity and accuracy of expression presented here, one can easily calculate the values of the AFD using a scientific calculator since it does not require complicated mathematical transformations of sophisticated functions, and since the ABC algorithm is robust and convenient, any expression can easily be constructed for different parameters such as elastic modulus, pore size, and porosity of different composite materials used for tissue scaffold.

Acknowledgment

This research was supported by Mersin University, Department of Scientific Research Projects with the project number of 2017-2-TP2-2495. We are thankful to Mersin University, Department of Scientific Research Projects.

References

[1] A. J. Salgado, O. P. Coutinho, and R. L. Reis, "Bone Tissue Engineering: State of the Art and Future Trends," Macromol Biosci., vol. 4, pp. 743-765, Aug. 2004.

[2] R. Murugan and S. Ramakrishna, "Development of nanocomposites for bone grafting," Compos Sci Technol., vol. 65, pp. 2385-2406, Dec. 2005.

[3] L. Bia, M. N. Rahamanb, D. E. Dayb, Z. Browna, C. Samujhc, X. Liub, A. Mohammadkhahb, V. Dusevicha, J. D. Eicka, and L. F. Bonewalda, "Effect of bioactive borate glass microstructure on bone regeneration, angiogenesis, and hydroxyapatite conversion in a rat calvarial defect model," Acta Biomater., vol. 9, pp. 8015-8026, Aug. 2013.

[4] H.-M. Lin, Y.-H. Lin, and F.-Y. Hsu, "Preparation and characterization of mesoporous bioactive glass/polycaprolactone nanofibrous matrix for bone tissues engineering," J Mater Sci-Mater M. vol. 23, pp. 2619-2630, Nov. 2012.

[5] F. J. O'brien, "Biomaterials & scaffolds for tissue engineering," Mater Today. vol. 14, pp. 88-95, Mar. 2011.

[6] B. P. Chan, and K.W. "Scaffolding in tissue engineering: general approaches and tissue-specific considerations," Leong, Eur Spine J. vol. 17, pp. 467-479, Dec. 2008.

[7] T. Gong, J. Xie, J. Liao, T. Zhang, S. Lin, and Y. Lin., "Nanomaterials and bone regeneration," Bone Res. vol. 3, Nov. 2015.

[8] L. Zhang, and T.J. Webster, "Nanotechnology and nanomaterials: Promises for improved tissue regeneration,"Nano Today. vol. 4, pp. 66-80, Feb. 2009.

[9] J. S. Grahama, A. N. Vomund, C. L. Phillips, and M. Grandbois, "Structural changes in human type I collagen fibrils investigated by force spectroscopy," Exp Cell Res. vol. 299, pp. 335-342, Oct. 2004.

[10] F. Zamani, M. A. Tehran, M. Latifi, and M. A. Shokrgozar, "The influence of surface nanoroughness of electrospun PLGA nanofibrous scaffold on nerve cell adhesion and proliferation," J Mater Sci-Mater M. vol. 24, pp. 1551-1560, June. 2013.

[11] K. M. Woo, V.J. Chen, and P.X. Ma, "Nano-fibrous scaffolding architecture selectively enhances protein adsorption contributing to cell attachment," J Biomed Mater Res A. vol. 67, pp. 531-537, Nov. 2003.

[12] E. Vatankhaha, D. Semnania, M. P. Prabhakaranb, M. Tadayonc, S. Razavid, and S. Ramakrishna, "Artificial neural network for modeling the elastic modulus of electrospun polycaprolactone/gelatin scaffolds,"Acta Biomater. vol. 10, pp. 709-721, Feb. 2014.

[13] K. Nasouri, A. Shoushtari, and M. Mojtahedi, "Effects of polymer/solvent systems on electrospun polyvinylpyrrolidone nanofiber morphology and diameter," Polym Sci Ser A+. vol. 57, pp. 747-755, Nov. 2015.

[14] J.-H. Jang, O. Castanod, H.-W. Kim, "Electrospun materials as potential platforms for bone tissue engineering," Adv Drug Deliver Rev. vol. 61, pp. 1065-1083, Oct. 2009.

[15] E. I. Paşcu, J. Stokes, and G.B. McGuinness, "Electrospun composites of PHBV, silk fibroin and nano-hydroxyapatite for bone tissue engineering," Mat Sci Eng C-Mater. vol. 33, pp. 4905-4916, Dec. 2013.

[16] S. Heydarkhan-Hagvalla, K. Schenke-Laylandb, A. P. Dhanasopona, F. Rofaila, H. Smitha, B. M. Wuc, R. Shemina, R. E. Beyguia, and W. R. MacLellanb, "Three-dimensional electrospun ECM-based hybrid scaffolds for cardiovascular tissue engineering," Biomaterials. vol. 29, pp. 2907-2914, July. 2008.

[17] C. Gao, M. N. Rahaman, Q. Gao, A. Teramoto and K. Abe, "Robotic deposition and in vitro characterization of 3D gelatin−bioactive glass hybrid scaffolds for biomedical applications," J Biomed Mater Res A. vol. 101, pp. 2027-2037, July. 2013.

[18] C. Gao, Q. Gao, Y. Li, M. N. Rahaman, A. Teramoto, and K. Abe, "In vitro evaluation of electrospun gelatin-bioactive glass hybrid scaffolds for bone regeneration," J Appl Polym Sci. vol. 127, pp. 2588-2599, Feb. 2013.

[19] S. Ö. Gönen, B. Ertürk, E. Tüccar, M. E. Taygun, and S. Küçükbayrak, "Effects of electrospinning parameters on gelatin/bioactive Glass nanofiber diameter," Anadolu University Journal Of Science And Technology–A Applied Sciences and Engineering. vol. 16, pp. 135-144, Nov. 2015.

[20] X. Li, L. Wang, Y. Fan, Q. Feng, F.-Z. Cui, and F. Watari, "Nanostructured scaffolds for bone tissue engineering," J Biomed Mater Res A. vol. 101, pp. 2424-2435, Aug. 2013.

[21] S.M.S Mahdi, A. Kheradmand, V. Montazeri, and H. Ziaee, "Effects of process and ambient parameters on diameter and morphology of electrospun polyacrylonitrile nanofibers," Polym Sci Ser A+. vol. 57, pp. 155-167, Mar. 2015.

[22] H. M. Khanlou, A. Sadollah, B. C. Ang, J. H. Kim, S. Talebian, and A. Ghadimi, "Prediction and optimization of electrospinning parameters for polymethyl methacrylate nanofiber fabrication using response surface methodology and artificial neural networks," Neural Comput Appl, vol. 25, pp. 767-777, Sep. 2014.

[23] S. Mohammadzadehmoghadam, Y. Dong, and I. J. Davies, "Modeling electrospun nanofibers: An overview from theoretical, empirical, and numerical approaches," Int J Polym Mater. vol. 65, pp. 901-915, May. 2016.

[24] M. Naghibzadeh, and M. Adabi, "Evaluation of effective electrospinning parameters controlling gelatin nanofibers diameter via modelling artificial neural networks," Fiber Polym. vol. 15, pp. 767-777, Apr. 2014.

[25] K. Nasouri, H. Bahrambeygi, A. Rabbi, A. M. Shoushtari, and A. Kaflou, "Modeling and optimization of electrospun PAN nanofiber diameter using response surface methodology and artificial neural networks," J Appl Polym Sci. vol. 126, pp. 127-135, Oct. 2012.

[26] M.P. Modaress, H. Mirzadehb, and M. Zandia, "Gelatin–GAG electrospun nanofibrous scaffold for skin tissue engineering: Fabrication and modeling of process parameters," Mater Sci Eng C Mater Biol Appl. vol. 48, pp. 704-712, Mar. 2015.

[27] Pezeshki-Modaress, M., M. Zandi, and H. Mirzadeh, "Fabrication of gelatin/chitosan nanofibrous scaffold: process optimization and empirical modeling," Polym Int. vol. 64, pp. 571-580, Apr. 2015.

[28] S. Khalili, S. N. Khorasani, N. Saadatkish, and K. Khoshakhlagh, "Characterization of gelatin/cellulose acetate nanofibrous scaffolds: Prediction and optimization by response surface methodology and artificial neural networks," Polym Sci Ser A+. vol. 58, pp. 399-408, May. 2016.

[29] M. Yazdimamaghani, D. Vashaee, S. Assefa, K. J. Walker, S. V. Madihally, G. A. Köhler, and L. Tayebi, "Hybrid Macroporous Gelatin/Bioactive-Glass/Nanosilver Scaffolds with Controlled Degradation Behavior and Antimicrobial Activity for Bone Tissue Engineering," J Biomed Nanotechnol. vol 10, pp. 911-931, June. 2014.

[30] T. Qu, and X. Liu, "Nano-structured gelatin/bioactive glass hybrid scaffolds for the enhancement of odontogenic differentiation of human dental pulp stem cells," J Mater Chem. vol. 1, pp. 4764-4772, July. 2013.

[31] M. Mozafari, M. Rabiee, M. Azami, and S. Maleknia, "Biomimetic formation of apatite on the surface of porous gelatin/bioactive glass nanocomposite scaffolds," Appl Surf Sci. vol. 257, pp. 1740-1749, Dec. 2010.

[32] D. Karaboga, and B. Akay, "A comparative study of Artificial Bee Colony algorithm," Appl Math Comput. vol. 214, pp. 108-132, Aug. 2009.

[33] B. Nozohour-leilabady, and B. Fazelabdolabadi, "On the application of artificial bee colony (ABC) algorithm for optimization of well placements in fractured reservoirs; efficiency comparison with the particle swarm optimization (PSO) methodology," Petroleum. vol. 2, pp. 79-89, Mar. 2016.

[34] Z. Li, Z. Zhou, X. Sun, and D. Guo, “Comparative study of artificial bee colony algorithms with heuristic swap operators for traveling salesman problem,” in Intelligent Computing Theories and Technology, 2013, vol. 7996 pp. 224-233.

[35] D. Karaboga, and B. Basturk, "A powerful and efficient algorithm for numerical function optimization: artificial

bee colony (ABC) algorithm," J Global Optim. vol. 39, pp. 459-471, Nov. 2007.

BIOGRAPHIES

Cagdas Yılmaz was born in Mersin, Turkey, on 19 May 1991. He graduated from the Biomedical Engineering Department at Erciyes University, in 2014. In the following year, he started his MA in the Electrical-electronics engineering at Mersin University.

Deniz Ustun was born in Eregli–Konya, Turkey, on 26 April 1976. He received the B. Sc. degree in computer science engineering from the Istanbul University, Istanbul, Turkey, in 2001, and M.Sc. degree in department of electrical-electronics engineering from the University of Mersin, Turkey, 2009. Since 2010, he has been working toward the Ph.D. degree at the same department in Mersin University. Currently, he has been a senior lecturer in the department of software engineering, Tarsus Technology Faculty, Mersin University for three years. Mr. Ustun's research interests include the nature–inspired optimization techniques (genetic algorithm, ant colony optimization, differential evolution, particle swarm optimization, artificial bee colony, firefly, bat algorithms), algorithms and theory of computation, data mining, artificial neural network and support vector machine, ISAR imaging, computer modeling and simulation (microstrip antennas, computational electromagnetic), and applications of optimization algorithms to an electromagnetic problem such as radiation, resonance, and bandwidth.

Ali Akdagli received his B.S., M.S., and Ph.D. degrees in Electronic Engineering from Erciyes University, Kayseri, in 1995, 1997, and 2002, respectively. From 2003 to 2006, he was an Assistant Professor in the Electronic Engineering Department at Erciyes University. He joined the same department at Mersin University, where he currently works as a Professor. He has published more than 90 papers in journals and conference proceedings. His current research interests include evolutionary optimization techniques (genetic algorithm, ant colony optimization, differential evolution, particle swarm optimization, and artificial bee colony algorithms), artificial neural networks and their applications to electromagnetic, wireless communication systems, microwave circuits, microstrip antennas, and antenna pattern synthesis problems. Dr. Akdagli is an editorial board member of “Recent Patents on Electrical Engineering”, “International Journal of Computers”, and “Journal of Computational Engineering”.